Received: 19 December 2024 | Accepted: 2 September 2025

DOI: 10.1002/saj2.70141

Soil Science Society of America Journal

ORIGINAL ARTICLE

Fundamental Soil Science

Correlation of total organic C, particulate and mineral-associated C fractions with strength indicators in Oxisols

Renato P. de Lima[1,2] | Cassio A. Tormena[3] | Rafael B. Menillo[1] | Newton La Scala Júnior[4] | Anderson R. da Silva[5] | Zigomar M. Souza[2] | Carlos E. P. Cerri[1] | Maurício R. Cherubin[1]

[1]Department of Soil Science, Luiz de Queiroz College of Agriculture, University of São Paulo, Piracicaba, São Paulo, Brazil

[2]Agricultural Engineering College (FEAGRI), University of Campinas, Campinas, São Paulo, Brazil

[3]Department of Agronomy, State University of Maringá, Maringá, Paraná, Brazil

[4]Department of Exact Sciences, State University of São Paulo (UNESP), PPG-Ciência do Solo, Jaboticabal, São Paulo, Brazil

[5]Statistics and Geoprocessing Laboratory, Agronomy Department, Goiano Federal Institute, Urutai, Goiás, Brazil

Correspondence

Renato P. de Lima, Agricultural Engineering College (FEAGRI), University of Campinas, Campinas, São Paulo, Brazil.
Email: rplima@unicamp.br

Assigned to Associate Editor Robert Heinse.

Funding information

Conselho Nacional de Desenvolvimento Científico e Tecnológico, Grant/Award Number: 405784/2023-6; Fundação de Amparo à Pesquisa do Estado de São Paulo, Grant/Award Number: 2020/15783-4

Abstract

The specific role of each fraction of soil C (i.e., particulate [POC] or mineral-associated organic carbon [MAOC]) in each soil strength mechanism remains unexplored. We investigated the relationships of total organic C and its physical fractions with soil strength of two tropical soils (sandy clay loam [SCL_{soil}] and sandy clay [SC_{soil}]). We measured soil strength indicators from oven-dry aggregates [tensile strength (σ_t)] and some related to soil compaction [precompression stress (σ_p), compression index (λ), and penetration resistance (SPR) at constant matric potential (−100 hPa)]. These soil strength indicators were used as response variables in path analyses to determine direct effects of C, MAOC, and POC mediated by key physical strength inducers (bulk density or water content). Results suggest a C role conferring soil strength verified by positive correlation with tensile strength and SPR increase, positively influenced by MAOC in SCL_{soil} and C/POC/MAOC in SC_{soil}. For SPR, the C effect was mediated by water content or bulk density (i.e., indirect contribution for correlation). Organic C, in turn, showed limited effect on soil compressibility. These findings indicate that increases in soil carbon that enhance aggregate mechanical strength and penetration resistance do not result in reduced soil compressibility (i.e., resistance to compaction). In sandy clay loam soils, MAOC plays a key role in increasing soil strength, whereas all carbon fractions contribute to strength gains with increasing clay content. Thus, while organic carbon can promote beneficial structural stability in the long term, it may also increase SPR, which affects root growth.

Plain Language Summary

Healthy soil is important for growing crops, and part of what keeps soil strong is the amount of organic carbon it has. But not all carbon in the soil works the same way. In

Abbreviations: BD, bulk density; ECL, eucalyptus land use; ICL, integrated crop-livestock system; MAOC, mineral-associated organic carbon; NF, native forest; PA, pasture; POC, particulate organic carbon; SPR, soil penetration resistance; σ_p, precompression stress (kPa); σ_t, tensile strength of aggregates (kPa); λ, compression index.

this study, we looked at two types of tropical soils to understand how different kinds of carbon help the soil stay firm and resist being pressed down. We found that carbon attached to tiny minerals helps the soil stay strong, especially in sandy soils. In a clay soil, all types of carbon helped. But even when carbon made the soil stronger, it did not always stop it from getting compacted. This means that adding more carbon can be good for soil structure, but it might also make it harder for plant roots to grow. These results help us better manage soil to grow food in a healthy and sustainable way.

1 | INTRODUCTION

Soil strength is the capacity of a soil body or individual aggregates to withstand forces without experiencing failure, including rupture, fragmentation, and compression (Hillel, 2003; Horn & Fleige, 2011; Schjønning et al., 2015). In agricultural soil, strength results from the balance between forces responsible for its aggregation and those that cause aggregate breakdown or soil structure failure. Soil fails when stress levels exceed soil strength (Dexter et al., 1988). Mechanical stress is common external forces responsible for soil failure. A typical condition that leads to compressive stress is the force applied by agricultural vehicles and animals (Horn, 2004).

Soil structure strength can be evaluated using individual aggregates (e.g., tensile strength) or undisturbed soil cores (e.g., penetration resistance or compressibility). These soil strength indicators have agricultural applications for tillage fragmentation efficiency, soil furrow opening, crack formation, resistance to erosion, resistance to compression, and soil penetration resistance (SPR) to root development (Cavalcanti et al., 2020; Dexter & Watts, 2000; Imhoff et al., 2002; Moraes et al., 2017).

Organic matter inputs can induce microaggregate stabilization when incorporated into micropores (Dexter et al., 1988; Lavallee et al., 2020; Six et al., 2004), conferring soil strength. However, when considering formation and persistence mechanisms, organic matter pools may contain a considerable distribution of substances and fractions that act differently on aggregates and mineral particle binding (Cambardella & Elliott, 1992; Cotrufo et al., 2022). Although the fractionation of some pools can be achieved chemically or physically, a simple way to fractionate organic carbon pools is physical fractionation into particulate (particulate organic carbon [POC]—lightweight fragments relatively undecomposed) and mineral-associated (MAOC—chemical bonds between C and mineral surfaces/occlusion within micropores) (Prairie et al., 2023). Unlike POC, MAOC receives protection from decomposition by its association with soil minerals (Lavallee et al., 2020). Thus, MAOC tends to persist for much longer (decades/centuries) than POC (<10 years/decades), while POC is susceptible to soil tillage (Pesch et al., 2020).

Research suggests that mechanical stability increases with increasing organic matter (Cavalcanti et al., 2020; Horn, 2004; Moraes et al., 2017). Some authors argue that this strength gain would be induced by the strengthening of carbon bonds over time without soil mobilization, in a phenomenon called "age-hardening" (Dexter, 1990; Moraes et al., 2017). Based on these previous studies, "age-hardening" is a hypothesis that could explain strength gain via C input over time in land use systems without soil mobilization caused by tillage. According to Moraes et al. (2017), this strength gain occurs with negligible changes in water content or bulk density (BD). However, it remains unclear whether particulate or mineral-associated organic matter has any major influence on strength, since these studies evaluated total organic carbon.

Pesch et al. (2020) suggested that precompression stress increased due to greater amounts of particulate organic matter. Startsev et al. (2020) physically fractionated organic matter and studied soil compressive behavior, concluding that the lighter or lower density fraction provided greater structural soil stability and increased elasticity and resilience. The light fractions of organic matter are probably bound to soil particles, functioning as a structural strengthening factor (Startsev et al., 2020). Kunde et al. (2018) observed a reduction in the tensile strength of aggregates as total C in the soil reduced, whereas Stumpf et al. (2018) found no effect (including variations in the physical fraction of C) in aggregates measured under air-dried conditions. These results contrast with those reported by Moraes et al. (2017, 2019), who observed an increase in soil strength with time reinforcement of organic carbon bonds.

While organic carbon is widely recognized for stabilizing soil structure and improving soil health, its role in structural hardening, particularly in root penetration resistance and load-bearing capacity to mitigate soil compaction, remains poorly understood. However, it is unclear whether this effect is driven by particulate organic carbon—which promotes aggregate formation—or mineral-associated carbon—which provides long-term stability. Moreover, the relation between the predominant carbon fraction and soil resistance to compression and root growth lacks in-depth investigation. Understanding this dynamic is essential for improving soil management in sustainable agricultural systems, thus reducing the negative impacts of compaction.

Given previous evidence that long-term undisturbed soils accumulate carbon and exhibit increased mechanical strength (Horn, 2004; Moraes et al., 2017, 2019), we hypothesize that organic carbon is positively associated with soil strength, particularly MAOC. To test this, we measured strength indicators in aggregates and undisturbed cores from two Brazilian Oxisols (sandy clay loam and sandy clay).

Core Ideas

- Organic carbon correlates positively with soil strength.
- Clay enhances the role of C in soil aggregate strength.
- Soil compressibility strength is minimally affected by C.
- Continuous C input increases soil penetration resistance in long-term systems.

2 | MATERIALS AND METHODS

2.1 | Location and characterization of the experimental sites

For this study, two soils were sampled in Southern and Southeastern Brazil (June 2022), located in Jardim Olinda (Paraná State) and Selvíria (Mato Grosso do Sul State), respectively. In Jardim Olinda, the samples were collected from a commercial farm (22°34′29.8″ S 52°03′24.3″ W), whereas in Selvíria the soil sampled belonged to an experimental farm at Universidade Estadual Paulista (UNESP) (20° 20′53.41″ S, 51° 23′55.50″ W). Both soils are classified as Oxisols (Soil Survey Staff, 2014), with sandy clay loam (Jardim Olinda—73% sand, 2% silt, and 25% clay) and sandy clay (Selvíria—60% sand, 3% silt, and 37% clay) textures. Henceforth, the two soils will appear as SCL_{soil} (from Jardim Olinda) and SC_{soil} (from Selvíria) in reference to their respective clay contents.

To achieve soil organic carbon variability (C total and its fractions), three contrasting land use sites were chosen in each location for investigating the impacts of organic carbon content on soil strength indicators. For SCL_{soil}, samples were collected in native forest (NF), integrated crop-livestock (ICL), and pasture (PA) systems, whereas for SC_{soil} the soil was sampled in NF, eucalyptus land use, and PA land uses (Table 1).

2.2 | Soil samplings

Five sampling points (i.e., five replicates) were randomly selected within each experimental site. After digging out a mini-trench (approximately 0.4 m × 40 m × 0.4 m) using a spade, undisturbed soil cores (5 cm diameter and 5 cm height) were taken at 0.0–10 cm (30 samples) and 10–20 cm (30 samples) depths, totalling 60 samples for both soils. These soil cores were used for penetration resistance and BD measurements. Additional 60 undisturbed cores (7 cm diameter and 2.5 cm height) were collected at 0.0–10 cm (30 samples) and 10–20 cm (30 samples) depth for soil compression tests in both soils. Finally, undisturbed soil blocks (10 cm × 10 cm × 10 cm) were collected at 0.0–10 cm and 10–20 cm for tensile strength tests. A basic flowchart of soil sampling locations and characteristics is shown in Figure 1.

2.3 | Laboratory measurements

2.3.1 | Tensile strength measurement

Undisturbed soil blocks were oven-dried at 45°C for 72 h. While Dexter and Kroesbergen (1985) recommended 105°C oven-dry of aggregates for testing, the 45°C oven-dry was used to homogenize aggregate moisture and to preserve organic matter from any alteration (Dexter et al., 1988). A subsample was sieved from each soil sample replicate for a mesh between 8.00 and 4.75 mm (i.e., 6.38 mm aggregates' mean diameter). In total, 20 oven-dried 6.38 mm aggregates were separated for tensile strength (σ_t) measurements. Thus, 200 aggregates were tested for each site, totaling 1200 aggregates (six sites, two depths, five replicates, and 20 aggregates per replicate). Determinations used the crushing method described by Dexter and Kroesbergen (1985), in which a digital crushing apparatus is placed where the aggregate under test is loaded between a bottom and upper plate connected to the loading transducer. Crushing force was applied until cracking. The maximum load value at the crack moment was then digitally recorded for calculating the tensile strength (σ_t) as follows (Dexter & Kroesbergen, 1985; Imhoff et al., 2002):

$$\sigma_t = 0.576\left(\frac{F}{D^2}\right) \quad (1)$$

$$D = D_m\left(\frac{M}{\bar{M}}\right)^{1/3} \quad (2)$$

in which 0.576 is the coefficient of proportionality, resulting from the relation between the applied compressive load and the tensile stress induced inside the aggregate; F is the force required for tensile cracking of the aggregate (N) and D is the effective diameter of the aggregate (m). Effective diameter (D) was calculated according to Equation (2), in which

TABLE 1 Historical land use description of experimental fields.

Soil	Soil/land use	Geographic coordinates	Historical land use description
Sandy clay loam	Native forest	22°33′45.2″ S, 52°05′22.2″ W	Land use under maintenance of native forest
	Integrated crop-livestock	22°33′56.8″ S, 52°03′36.1″ W	Cultivation was first implemented in 2010. From 2010 to 2012, it was managed under the crop-livestock sequence: (1) soybean, (2) maize intercropping with brachiaria, and (3) brachiaria-livestock. After 2012, the area has been managed with brachiaria, receiving annual limestone and organic poultry manure maintenance without soil tillage intervention.
	Pasture	22°34′36.4″ S, 52°03′23.6″ W	Currently cultivated with brachiaria since 1984, with just one production year (2005) where soybean was cultivated. Since 2005, there has been no tillage disturbance. Cattle make use of the area for grazing.
Sandy clay	Native forest	20°20′57.1″ S, 51°23′52.6″ W	Land use under maintenance of native forest
	Eucalyptus	20°21′00.5″ S, 51°23′52.9″ W	Soil cultivated with eucalyptus (*Eucalyptus camadulensis*) since 1986 with spacing of 4 × 4 m. Without soil tillage since eucalyptus implementation.
	Pasture	20°20′57.4″ S, 51°23′46.6″ W	Currently cultivated with brachiaria since 2007. Since 2007, there has been no tillage disturbance. Tillage for eucalyptus implementation was performed with plowing and harrowing. In 2019, the area received limestone and NPK fertilizer applied on soil surface. Cattle make use of the area for grazing.

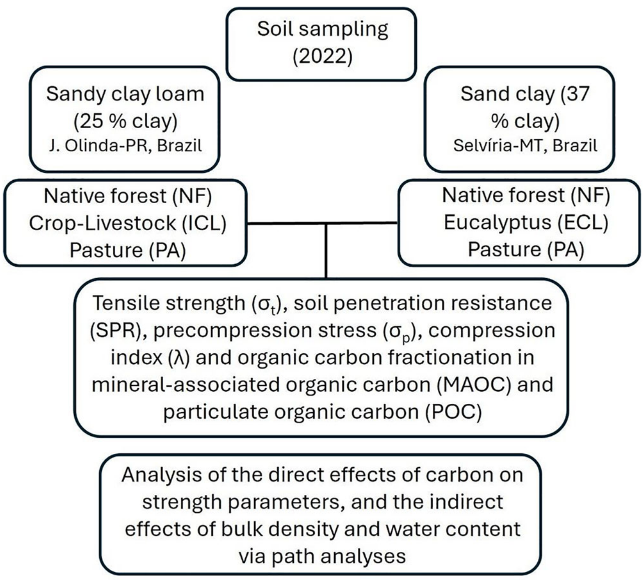

FIGURE 1 Basic flowchart of local soil sampling and characteristics, laboratory analysis, and data analysis.

D_m is the average diameter of the aggregate (mm), defined by the average of the sieve sizes (6.38 mm for this study); M is the mass of the individual aggregate (g); and $\bar{M}$ is the average mass of the aggregates representing each site, group, or treatment (g) according to Imhoff et al. (2002). Calculating the effective diameter therefore considers the average size of the aggregates passed through the sieve, the individual masses, and the population of aggregates examined to weigh the effect of mass and size on the average diameter. According to Dexter and Kroesbergen (1985), this method is especially effective since D_m is known and the masses can be quickly determined by weighing.

2.3.2 | SPRand compressibility measurements

All 5 cm diameter and 5 cm height soil cores were slowly saturated by capillarity rise for 48 h and then subjected to a matric potential of −100 hPa using Richards's apparatus. This matric potential was chosen to simulate the soil field capacity condition (van Lier, 2017). At hydraulic equilibrium, the soil cores were weighed for determining soil water content. Immediately after sample weighing, SPR tests were conducted in an electronic benchtop penetrometer (Brookfield model) at a speed of 10 mm/h and a cone semi-angle of 30°, for a tip diameter of 4 mm, and calculated as the average penetration resistance recorded for 2–4 cm of the height cores per Figueiredo et al. (2011). After testing, the cores were oven-dried at 105°C for 48 h. BD was calculated from the ratio between the mass of the oven-dried soil and total core volume.

For the 7 cm diameter and 2 cm height soil cores, confined uniaxial compression tests used an apparatus described by Figueiredo et al. (2011). Each of the following vertical stresses was applied for 5 s (5 s loading and unloading) in a sequential loading mode: 12.5, 25, 50, 100, 200, 400, and 800 kPa. As the rear wheels of a typical tractor moving at 5 m/h exert stress on the soil for <0.2 s (Or & Ghezzehei, 2002), this loading time was the fastest achievable with the apparatus used and simulated the brief loading duration of an agricultural tire during wheeling (Salire et al., 1994). Soil displacement was measured after each loading step by a displacement transducer and used for calculating changes in soil volume. After testing, the cores were oven-dried at 105°C for 48 h for soil BD calculation.

Precompression stress (σ_p) and compression index (λ) were calculated using the *sigmaP* function available in the *soilphysics* (R Core Team, 2022; da Silva & de Lima, 2016). σ_p was determined using the Pacheco Silva method (Toledo et al., 2021), the graphical illustration of which is given in da Silva and de Lima (2015) and Toledo et al. (2021). λ was estimated as the slope of the soil virgin compression line (Equation 3), fitted on the void ratio (ε)-$\log_{10}$ (stress) space over the soil compression curve, in which 400 and 800 kPa are the vertical stress levels applied in the uniaxial compression test.

$$\lambda = -\left[\frac{\varepsilon_{800} - \varepsilon_{400}}{\log_{10}(800) - \log_{10}(400)}\right] \tag{3}$$

2.3.3 | Organic carbon quantifications

Soil organic matter was physically fractionated into POC and mineral-associated organic matter (MAOC) following the particle-size method proposed by Cambardella and Elliott (1992). Aggregates between 8.00 and 4.75 mm from each sample were sieved through a 2.00-mm mesh. A 5 g of the sieved sample was dispersed with sodium hexametaphosphate in a horizontal shaker for 16 h. Subsequently, the dispersed solution was passed through a 53-µm mesh for separating POC (>53 µm) and MAOC (<53 µm). Both separated materials were oven-dried at 50°C and then ground and sieved through 100 mesh (<0.149 mm) for C quantification using an Elemental Analyzer–LECO/Truspec. Total C was calculated by adding the two C components, obtained from the POC and MAOC individual fractions.

2.4 | Data analyses

Analysis of variance (ANOVA) compared the strength indicators or organic carbon fractions between land uses considering the two textural classes (sand clay loam or sandy clay). Comparisons were performed separately for each layer (i.e., 0.0–0.1 or 0.1–0.2 m). Data were tested for normality and homogeneity of variances. Means were compared by Scott–Knott test.

Correlations between total organic C, its physical fractions, and soil strength indicators were examined using path analyses. Data from the three land uses and two sampled layers were used to achieve variability, considering BD and total C, POC, and MAOC as explanatory variables for tensile strength (σ_t), and BD, water content, and total C, POC, and MAOC as explanatory variables for compaction indicators (precompression stress [σ_p], compression index [λ], and SPR). We decomposed the total correlation of organic carbon components with soil strength indicators using path analysis to examine the indirect contributions of BD and water content, and the direct contribution of organic carbon components. The linear model for the correlation between variables SPR and C is specified in Equation (4). The models for all the other relations follow the same specification structure.

$$r_{C,SPR} = P_{C,SPR} + P_{POC,SPR}r_{POC,C} + P_{MAOC,SPR}r_{MAOC,C} + P_{BD,SPR}r_{BD,C} + P_{W,SPR}r_{W,C} \tag{4}$$

in which $r_{(.)}$ represents a Pearson's correlation, and $P_{(.)}$ represents a direct effect (path coefficient). Student's *t*-test was applied to check for significant non-null correlations at 5% significance level.

Variance inflation factor (VIF) tested variance inflation based on the correlation matrix of explanatory variables. Variables with VIF >5.0 were removed from the path analysis model (Akinwande et al., 2015; da Silva et al., 2013).

ANOVA, path analysis, and collinearity diagnostics (VIF) were performed on R (R Core Team, 2022) using the *biotools* package (da Silva et al., 2017).

3 | RESULTS

3.1 | BD and organic carbon components

BD was significantly higher for ICL and PA land uses than for NF in sandy clay loam soil (SCL_{soil}). ICL and PA obtained mean values of 1.73–1.67 Mg m^{-3}, whereas NV had a BD of 1.55–1.41 Mg m^{-3}. For sandy clay soil (SC_{soil}), ECL and PA also achieved the highest BD values (~1.69 Mg m^{-3}), which were significantly higher than those found in NV (1.50–1.44 Mg m^{-3}) (Table 2). Overall, the values indicated an increase in BD with agricultural land use.

PA fields obtained the highest total C average values in both soils (15–17 g kg^{-1}), followed by NV (11–12 g kg^{-1}) (Figure 2). As expected, we found the highest total C values at the 0.0- to 10-cm depth. SC_{soil} presented the highest C levels (17 g kg^{-1}) compared with SCL_{soil} (15 g kg^{-1}). MAOC averages were significantly higher in SC_{soil}, concentrated mainly in NV and PA land uses. In turn, POC was higher in SCL_{soil}, also concentrated in NV and PA. Overall, SCL_{soil} exhibited the highest POC values, whereas SC_{soil} concentrated the highest C and MAOC values (Figure 2). Table 2 summarizes the absolute mean values and standard deviations.

TABLE 2 Average and standard deviation of soil physical/strength parameters and organic carbon fractions across land use systems in two Brazilian soils.

Soil	Land use	Layer (m)	PD (Mg m^{-3})	BD (Mg m^{-3})	W_{SPR} (g g^{-1})	$W\sigma_p$ (g g^{-1})	MAOC (g kg^{-1})	POC (g kg^{-1})	C (g kg^{-1})	σ_t (kPa)	SPR (MPa)	σ_p (kPa)	Λ (−)
Sand clay loam	NF	0.0–0.1	2.64	1.41 ± 0.06[b]	0.12 ± 0.02[a]	0.13 ± 0.02[a]	6.4 ± 1.1	4.4 ± 1.6	10.8 ± 2.5	56 ± 9	1.4 ± 0.6	83 ± 17	0.30 ± 0.05
		0.1–0.2	2.70	1.55 ± 0.06[b]	0.11 ± 0.02[b]	0.10 ± 0.02[b]	4.4 ± 0.5	2.5 ± 0.2	6.9 ± 0.5	44 ± 6	1.6 ± 0.7	100 ± 31	0.25 ± 0.02
	ICL	0.0–0.1	2.70	1.72 ± 0.03[a]	0.15 ± 0.01[a]	0.15 ± 0.01[a]	6.9 ± 2.1	2.2 ± 0.8	9.1 ± 2.8	79 ± 15	3 ± 0.5	111 ± 26	0.13 ± 0.03
		0.1–0.2	2.68	1.67 ± 0.02[a]	0.13 ± 0.01[a]	0.15 ± 0.00[a]	5.3 ± 1.3	1.2 ± 0.3	6.5 ± 1.5	81 ± 15	2.3 ± 0.6	107 ± 35	0.28 ± 0.05
	PA	0.0–0.1	2.69	1.73 ± 0.05[a]	0.10 ± 0.01[b]	0.11 ± 0.02[b]	9.3 ± 1.1	5.4 ± 1.3	14.7 ± 1.1	80 ± 16	7.6 ± 1.7	90 ± 25	0.15 ± 0.06
		0.1–0.2	2.70	1.72 ± 0.06[a]	0.13 ± 0.01[a]	0.13 ± 0.02[a]	6.4 ± 0.8	3.2 ± 0.5	9.6 ± 1.1	80 ± 15	2.2 ± 0.5	120 ± 24	0.24 ± 0.10
Sandy clay	NF	0.0–0.1	2.74	1.50 ± 0.11[b]	0.20 ± 0.02[a]	0.21 ± 0.01[a]	13.2 ± 2.1	2.4 ± 0.9	15.6 ± 2.8	114 ± 33	1.5 ± 0.3	66 ± 9	0.43 ± 0.08
		0.1–0.2	2.73	1.44 ± 0.06[b]	0.21 ± 0.01[a]	0.22 ± 0.02[a]	10.1 ± 0.7	1.5 ± 0.2	11.6 ± 0.7	94 ± 15	1.2 ± 0.4	57 ± 17	0.43 ± 0.03
	ECL	0.0–0.1	2.76	1.54 ± 0.08[a]	0.15 ± 0.01[b]	0.14 ± 0.01[b]	8.3 ± 2.4	1.4 ± 0.4	9.7 ± 2.8	74 ± 15	2.1 ± 0.7	92 ± 26	0.27 ± 0.02
		0.1–0.2	2.72	1.69 ± 0.04[b]	0.16 ± 0.04[b]	0.17 ± 0.01[b]	6.3 ± 0.7	0.8 ± 0.2	7.1 ± 0.8	69 ± 15	2.1 ± 0.7	71 ± 13	0.29 ± 0.03
	PA	0.0–0.1	2.77	1.66 ± 0.09[a]	0.15 ± 0.03[b]	0.18 ± 0.01[b]	14.3 ± 1.5	3.0 ± 0.7	17.2 ± 1.9	120 ± 32	4.7 ± 2.3	93 ± 26	0.22 ± 0.08
		0.1–0.2	2.74	1.69 ± 0.04[a]	0.15 ± 0.03[b]	0.18 ± 0.03[b]	10 ± 1.2	2.0 ± 0.2	11.9 ± 1.4	123 ± 31	3.1 ± 1.4	75 ± 14	0.25 ± 0.09

Note: Averages do not differ for the same letter [in brackets] between land uses within soil textural class.

Abbreviations: BD, bulk density; C, organic carbon; ECL, eucalyptus; ICL, integrated crop-livestock system; MAOC, mineral-associated soil organic carbon; NF, native forest; PA, pasture; PD, particle density; POC, particulate soil organic carbon; SPR, soil penetration resistance; W_{SPR}, gravimetric water content at -100 hPa matric potential for SPR measurement; $W\sigma_p$, gravimetric water content at -100 hPa matric potential for σ_p measurement; λ, soil compression index; σ_p, precompression stress; σ_t, tensile strength.

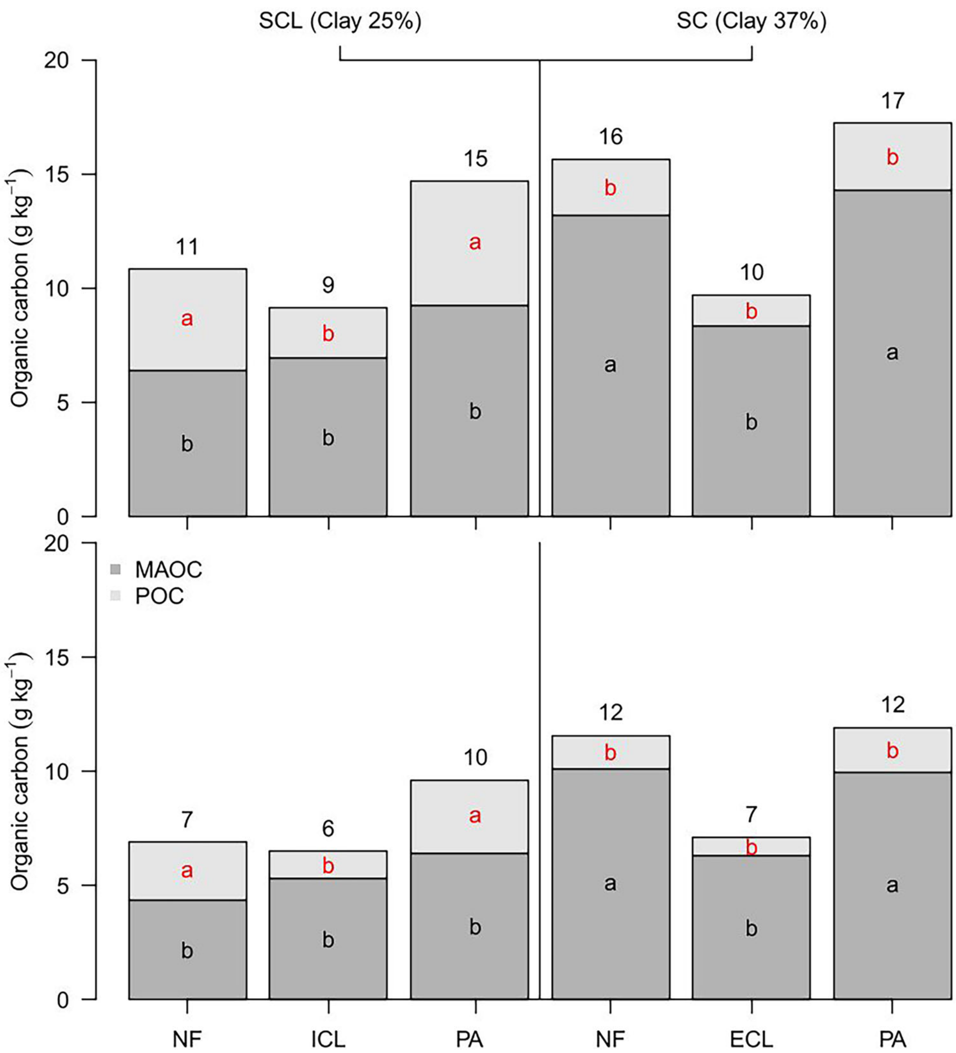

FIGURE 2 Proportion of mineral-associated organic carbon (MAOC) and particulate organic carbon (POC) in the total organic carbon of the C_{25}–sandy clay loam soil (25% clay) and C_{37}–sandy clay soil (37% clay). For C_{25}: native forest (NF), integrated crop-livestock (ICL), and pasture (PA). For C_{37}: native forest (NF), eucalyptus (ECL), and pasture (PA) land uses. SCL, sandy clay loam. Same letters do not differ by Scott–Knott test.

3.2 | Variability of soil strength indicators

SC_{soil} presented the higher tensile strength (σ_t) values, with averages ranging from 100 to 120 kPa (Table 2) in NV and PA. Averages for these land uses were significantly higher than for SCL_{soil} (Figure 3), which obtained average values of 80 kPa.

Only the 0.1–0.2 m layer of SCL_{soil} showed significantly higher values for precompression stress (σ_p), with averages ranging from 120 to 99 kPa in SCL_{soil} and from 57 to 75 kPa in SC_{soil} (Table 2). We observed no difference between soils or land use for the surface layer (Figure 4), with averages around 111–66 kPa. These results indicate no effect of land use on σ_p, only of soil (Figure 4). Native vegetation (NV) obtained the highest compression index (λ) values both on SCL_{soil} ($\lambda = 0.30$) and SC_{soil} ($\lambda = 0.43$) (Table 2). Overall, λ was highest in NV and lowest in PA lands. Unlike σ_p, land use influenced λ (Figure 5).

SPR was significantly higher in PA lands, regardless of soil texture (Figure 6). Average SPR values reached 7.6 MPa and 4.7 MPa for SCL_{soil} and SC_{soil}, respectively, and were higher in the surface layer (Table 2; Figure 6). For NF, the values did not exceed 2.0 MPa, whereas average values reached 3.0 MPa for eucalyptus. Overall, SPR values were higher for SCL_{soil}.

3.3 | Correlations of soil strength indicators with organic carbon components

Correlations between tensile strength (σ_t) and organic carbon components indicated that only MAOC correlated with σ_t in SCL_{soil} ($r = 0.36$) (Figure 7A), whereas all C components correlated with σ_t ($r \sim 0.55$) in SC_{soil} (Figure 7B), with no indirect effect of BD. However, BD contributed to the correlation with MAOC in SCL_{soil}, that is, soil BD enhanced

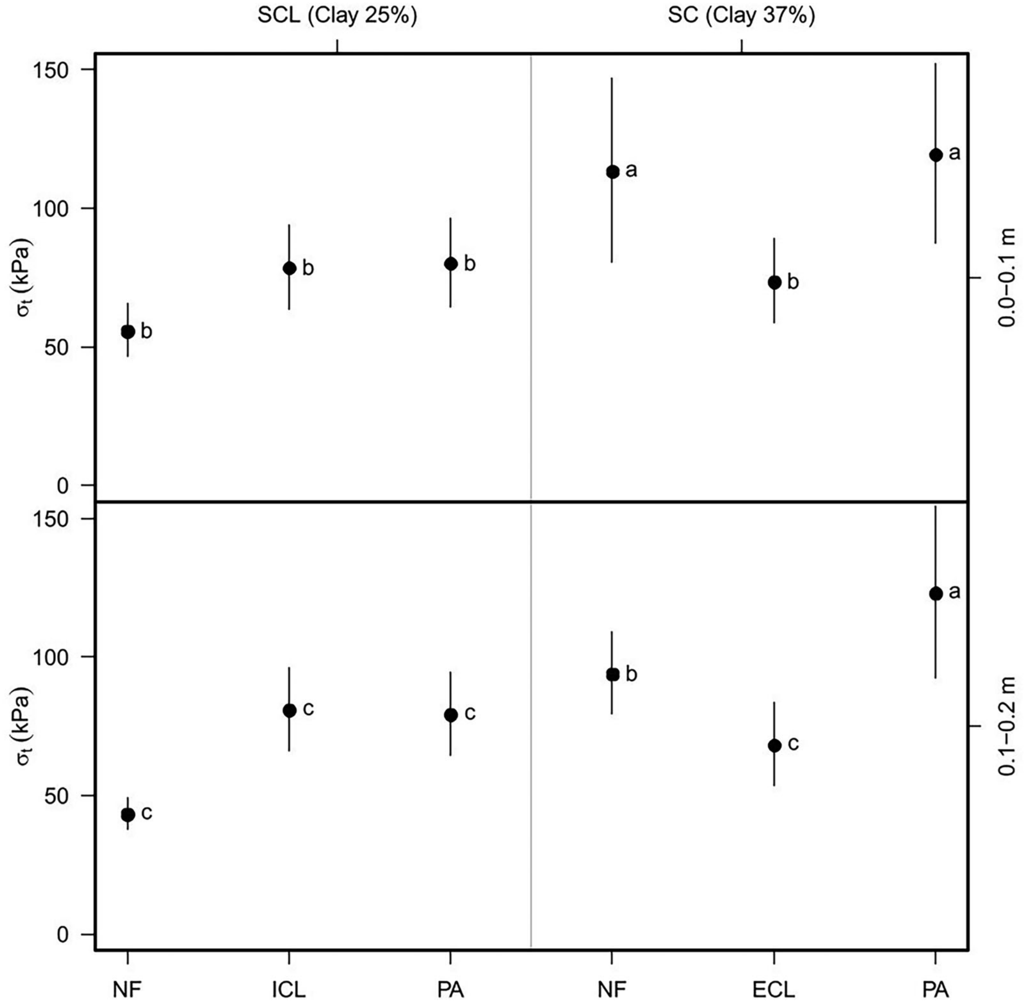

FIGURE 3 Comparison of tensile strength (σ_t) averages obtained in sandy clay loam (SCL) and sandy loam (SL) soil in different land uses and two layers. Same letters do not differ by Scott–Knott test. Vertical bars indicate standard deviation. ECL, eucalyptus; ICL, integrated crop-livestock system; NF, native forest; PA, pasture.

the tensile strength gain with increasing MAOC (46% contribution; Figure 7C). Only organic carbon indicated a positive effect on σ_t in SC_{soil}.

We found no correlation between precompression stress (σ_p) and the C components analyzed (Figure 8). A negative correlation ($r = -0.40$) between λ and MAOC was observed only for SCL_{soil} (Figure 9A). Path analyses found a contribution from water content (W) (27%) and from BD (5%) for the $\lambda \times$ MAOC correlation (Figure 9C). These results indicate a restricted impact of total organic carbon and its fractions on compressibility indicators, with effects observed only for soil compression index in SC_{soil} but with contributions from other physical variables.

SPR showed positive correlations with all C components, suggesting that increasing C increased SPR (Figure 10). However, W (21%–28%) and BD (8%–20%) contributed to these correlations in SCL_{soil}, and W (31%–35%) contributed to SPR gains in SC_{soil} (Figure 10C,D). For SCL_{soil}, this indicates that increases in soil C components promoted SPR gains mediated by increases in W and BD (Figure 10A), whereas for SC_{soil} increases in SPR induced by organic carbon were mediated by decreasing water content (Figure 10B). Of all the soil strength indicators analyzed, SPR proved to be the one with positive influence on organic carbon in both soils, but the SPR × organic carbon correlations were also mediated by key physical attributes responsible for variation in soil strength (W or BD).

4 | DISCUSSION

4.1 | C accumulation was significantly higher in PA lands

Carbon accumulation levels were higher in PA lands compared with the other land uses, showing numerically higher averages but statistically similar to NFs. This accumulation was greater in soil with higher clay content. Increased soil C

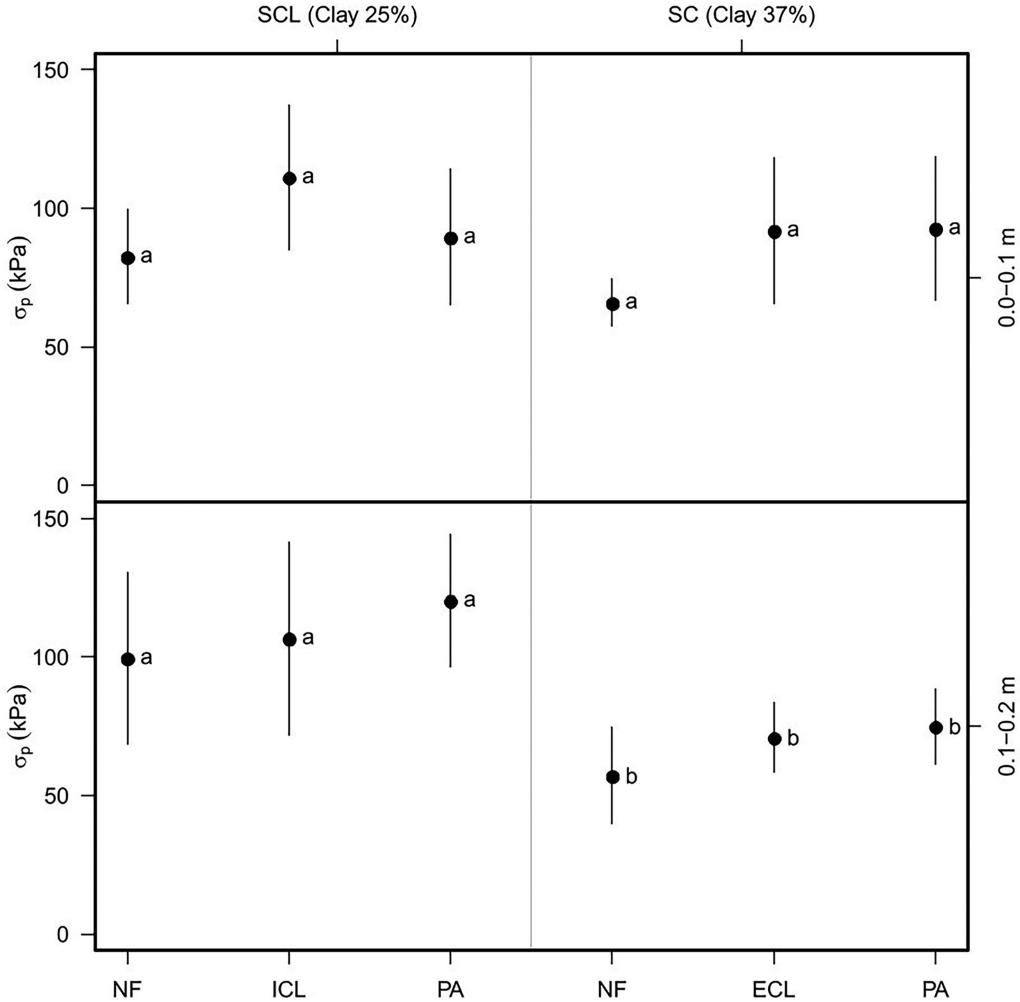

FIGURE 4 Comparison of precompression stress (σ_p) averages obtained in sandy clay loam (SCL) and sandy loam (SL) soil in different land uses and two layers. Same letters do not differ by Scott–Knott test. Vertical bars indicate standard deviation. ECL, eucalyptus; ICL, integrated crop-livestock system; NF, native forest; PA, pasture.

concentrations in surface layers are a common consequence of PA formation due to contributions from its root system exudates, volume, and intensive decomposition turnover (Cerri et al., 2018; Trumbore et al., 1995).

While C levels were similar between NF and PA, BD was significantly lower in NF compared with PA areas. But this difference did not result in variations in tensile strength between the two land uses, indicating that the tensile strength of NFs is comparable to that of PA in terms of carbon levels but not in BD. This difference was also reflected in the compression index, for which NFs achieved the highest values, whereas precompression stress showed no differences. This suggests that the higher porosity of NFs rather than carbon content may increase their susceptibility to compaction.

Penetration resistance was significantly higher in PA, where both carbon levels and BD were greater. Differences in SPR between land uses were most pronounced in the surface layer, despite the lack of variation in BD across PA layers in the two soils. This suggests that other resistance mechanisms contribute to increasing SPR in addition to BD.

4.2 | Clay content enhances the role of organic carbon as a driver of aggregate strength

In our study, carbon shows a contribution to soil strength considering the variability of all treatments. Aggregate tensile strength was positively correlated with all measured carbon pools for the SC_{soil}, whereas only mineral-associated organic carbon contributed to increased tensile strength in the sandy clay loam soil. However, soil BD was an important factor mediating tensile strength increase in this soil. These results suggest that total C (particulate + mineral-associated C) contributed to the strength of soil aggregates in the presence of larger clay amounts (i.e., SC_{soil}), as also observed by Bin and Xin-Hua (2006). This correlation of carbon components with tensile strength in soil with higher clay content may stem

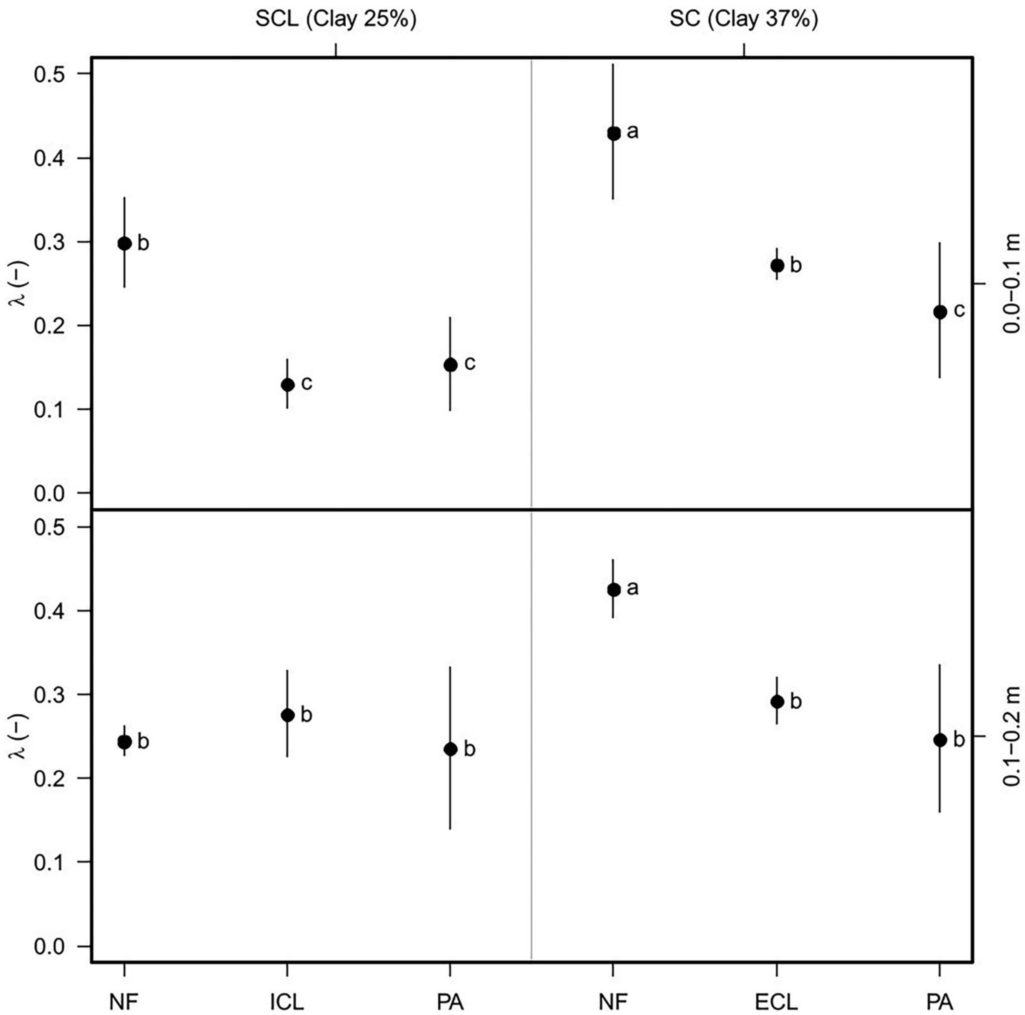

FIGURE 5 Comparison of soil compression index (λ) averages obtained in sandy clay loam (SCL) and sandy loam (SL) soil in different land uses and two layers. Same letters do not differ by Scott–Knott test. Vertical bars indicate standard deviation. ECL, eucalyptus; ICL, integrated crop-livestock system; NF, native forest; PA, pasture.

from increased specific surface area of soil particles, which is enhanced by the amount of sesquioxides typical of Oxisols. Singh et al. (2017) observed that soil carbon stabilization of aggregates was more strongly associated with sesquioxide content than with clay types or their specific surface areas. Blanco-Moure et al. (2012) reported significant interactions between clay and organic carbon. Soils with the highest clay and organic carbon values indicated a considerable increase in aggregate strength, aligning with our data.

In turn, our findings suggest that the development of aggregates tensile strength under sandy soil demands carbon stabilization (MAOC) and increased BD. This indicates that in addition to MAOC, the labile fraction of organic carbon (POC), of frequent turnover (Lavallee et al., 2020; Six et al., 2004), contributes to aggregates stability and tensile strength without BD increase in soils with higher clay content, whereas an increase in soil BD and organic carbon stabilization (i.e., MAOC) seems to be necessary to induce tensile strength when clay content is lower.

According to Lavallee et al. (2020), MAOC contributes to stabilize both macro- and microaggregates, whereas other evidence indicates POC contribution only to the stabilization of macroaggregates >250 μm. As indicated by Lavallee et al. (2020), our results suggest that in macroaggregates (used for testing), both MAOC and POC control aggregate resistance mechanisms mainly for soil with higher clay content (Islam et al., 2022). In weathered tropical soils, Imhoff et al. (2002) argue that clay fraction consists of several Fe and Al oxides, which are known to interact with organic matter, providing increased soil tensile strength. As in our study, Imhoff et al. (2002) report a positive effect of total organic carbon with increasing clay content. Additionally, our findings suggest that the effect on strength gains seems to be induced either by POC or MAOC. Bin and Xin-Hua (2006) also observed a positive effect of POC and MAOC on aggregate stability in soils under reforestation.

By definition, particulate organic matter is a carbon fraction that is not associated with minerals (Cambardella & Elliott,

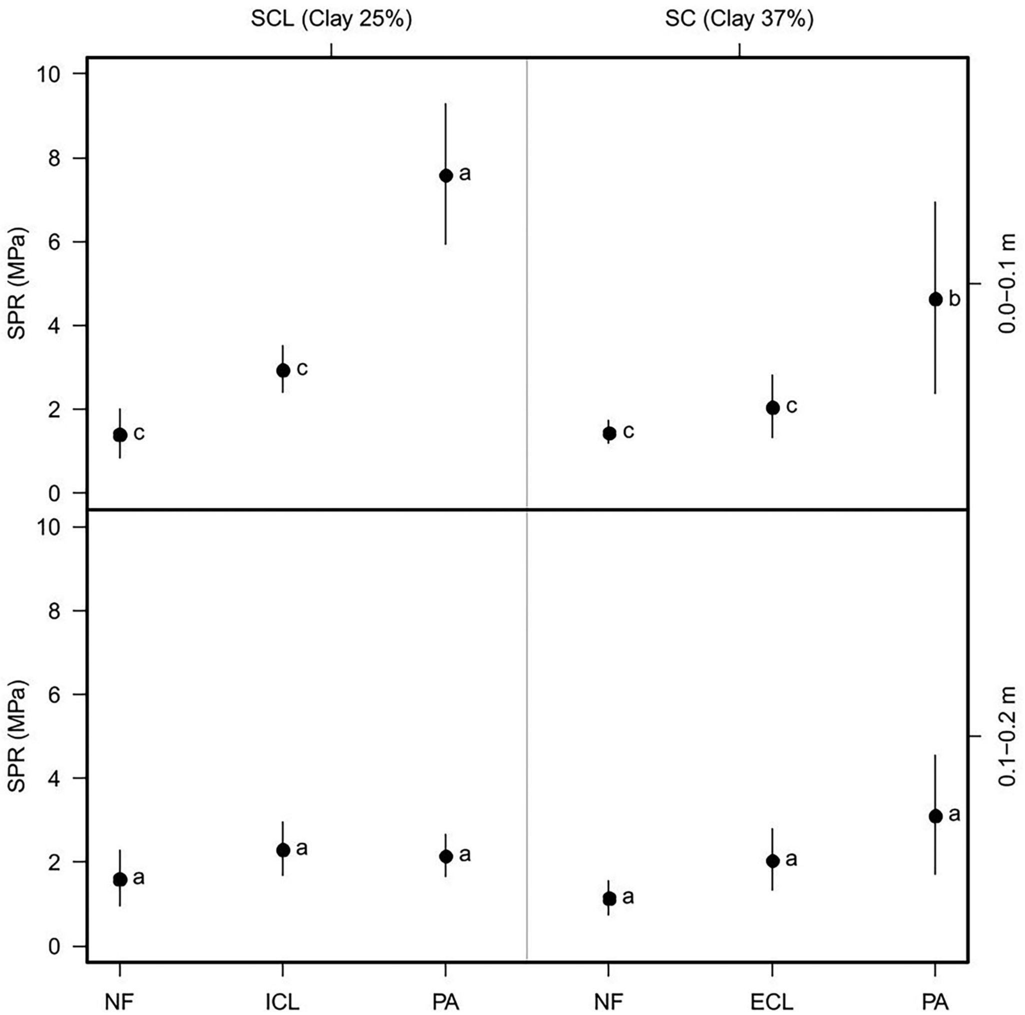

FIGURE 6 Comparison of soil penetration resistance (SPR) averages obtained in sandy clay loam (SCL) and sandy loam (SL) soil in different land uses and two layers. Same letters do not differ by Scott–Knott test. Vertical bars indicate standard deviation. ECL, eucalyptus; ICL, integrated crop-livestock system; NF, native forest; PA, pasture.

1992; Lavallee et al., 2020). Its protection mechanism relies on occlusion in large aggregates (Lavallee et al., 2020). Our results indicate that possible POC occlusion within the aggregates did not confer significant aggregate strength to the sandy clay loam soil. However, even with the smaller amount of clay, interaction of organic matter with the mineral fraction increased soil strength, the correlation of which was positively significant with MAOC. While soil strength development as a function of soil C was observed in the SC_{soil}, tensile strength was greater in the sandy clay loam soil (Table 2). This indicates that the presence of mineral-associated organic carbon can induce soil strength, but the likely number of interaction bonds between organic carbon and clay minerals is a key factor for soil strength gain, as reported by Moraes et al. (2017, 2019). Our results suggest that MAOC proportion is higher in SC_{soil} and that presence of this C fraction could be maintained in the absence of soil mobilization (Dexter, 1988).

Besides the association between soil organic carbon and clay minerals, soil BD partially drove soil tensile strength increase in the sandy clay loam soil (noted by the contribution of BD to the total correlation between C and tensile strength; Figure 7A). Similar contribution was not detected in the SC_{soil}, even though both soils presented a similar range of soil BD that allowed a wide variability in measurements. Soil BD affects soil strength due to an increase in the friction forces between soil particles (Imhoff et al., 2002) and an increased proportion of smaller pores in the soil (Błażejczak et al., 1995; Hadas & Lennard, 1988).

4.3 | Soil compressibility indicators were minimally affected by organic carbon

Organic carbon exhibited an effect on soil compression index only in the sandy clay loam soil, and this influence was indirectly mediated by soil BD and water content. Path analyses showed that these physical factors contributed to the correlation between mineral-associated organic carbon and

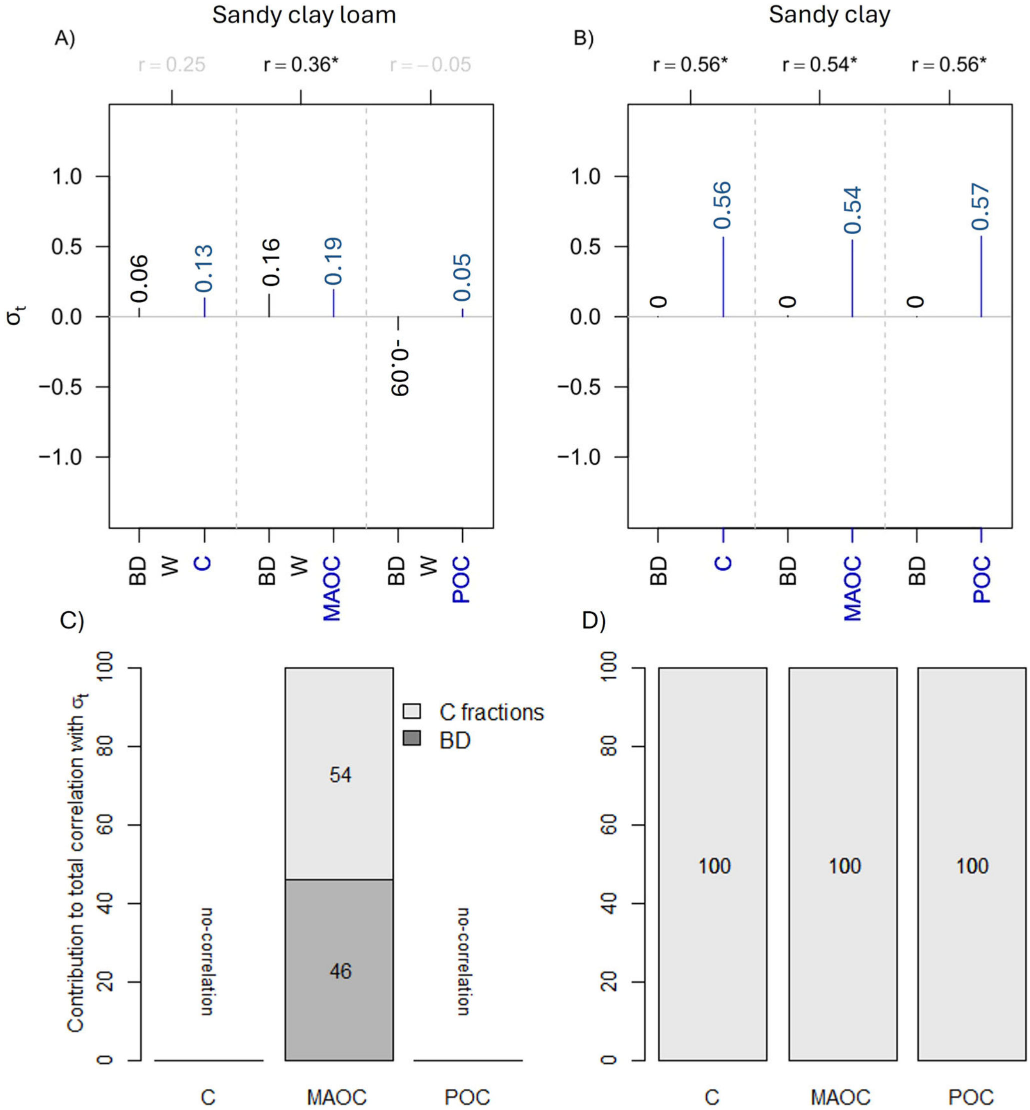

FIGURE 7 (A and B) Correlation (r) between the response variable σ_t (tensile strength) and total organic carbon and its fractions (organic carbon [C], mineral-associated organic carbon [MAOC], and particulate organic carbon [POC]). *$p < 0.05$. Vertical lines represent the estimates of path analysis coefficients. Blue lines indicate direct effects on σ_t. Black lines indicate indirect effects of soil bulk density (BD) through each carbon fraction on the correlation for the sandy loam soil and sandy clay soil. (C and D) Percentage contribution of path analysis coefficients to the correlation between σ_t and each C fraction.

compressibility. These results are similar to those found for aggregate measurements, where mineral-associated organic carbon played a role in tensile strength gains. However, organic carbon components presented no correlation with precompression stress or compression index for the SC_{soil}, contrasting with the results observed for the aggregate measurements. In correlations performed for organic carbon versus soil compressibility indicators (Table 3), both σ_p and λ significantly correlated with soil BD or water content, as also reported by Saffih-Hdadi et al. (2009), Schjønning and Lamandé (2018), and Toledo et al. (2021). This indicates that the pore system (e.g., BD) and water content dominate soil compressibility (Keller et al., 2011), with a minor C effect.

TABLE 3 Correlation of precompression stress (σ_p) and soil compression index (λ) with bulk density or gravimetric water content.

Soil texture	Strength indicator	BD	W
Sandy clay loam	σ_p	0.29	0.06
	λ	−0.49*	0.13
Sandy clay	σ_p	0.26	−0.50*
	λ	−0.66*	0.56*

Abbreviation: BD, soil bulk density; W, gravimetric water content.
*Significant at 0.05 by Pearson's correlation.

Pereira et al. (2007) found an increase in soil compression index as a function of organic carbon content in Cambisols,

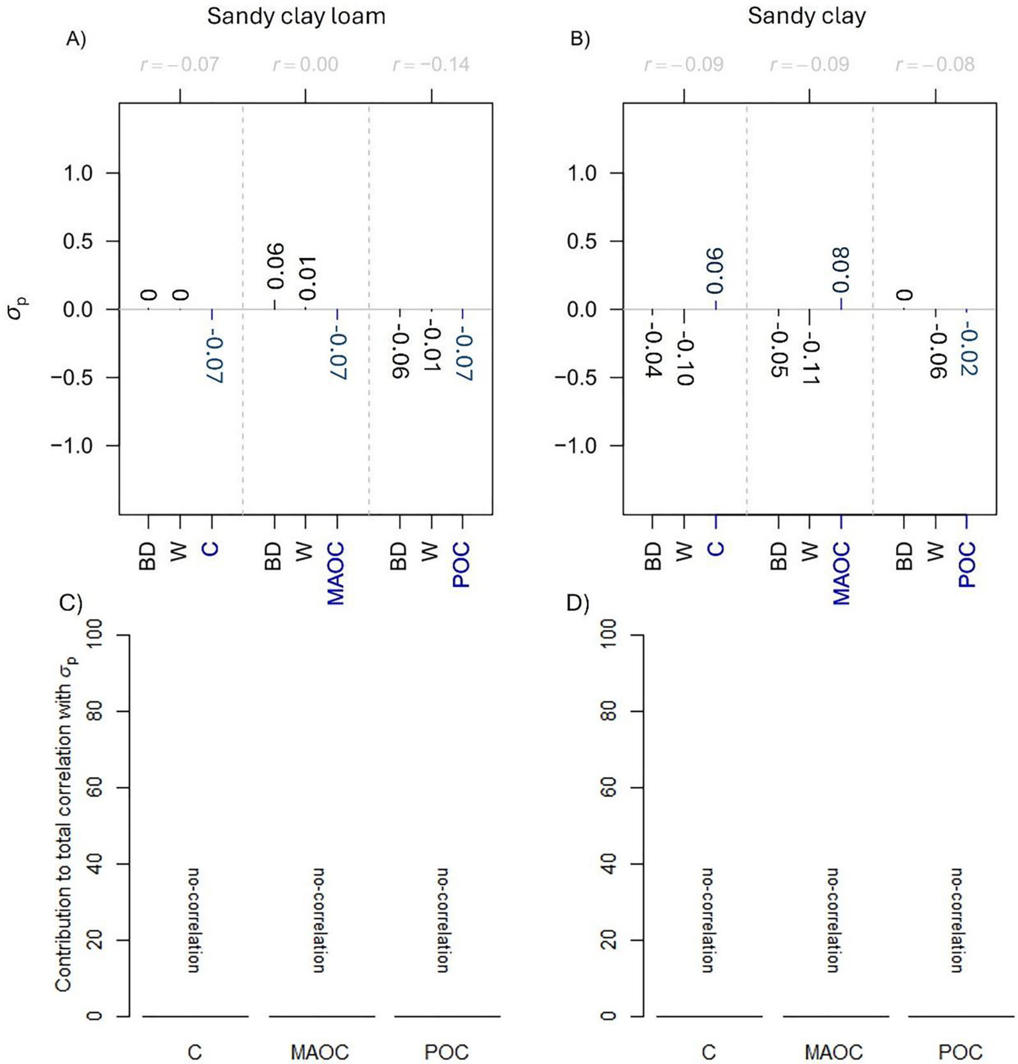

FIGURE 8 (A and B) Correlation (r) between the response variable σ_p (precompression stress) and total organic carbon and its fractions (organic carbon [C], mineral-associated organic carbon [MAOC], and particulate organic carbon [POC]). *$p < 0.05$. Vertical lines represent the estimates of path analysis coefficients. Blue lines indicate direct effects on σ_p. Black lines indicate indirect effects of soil bulk density (BD) and gravimetric water content (W) through each carbon fraction on the correlation for the sandy loam soil and sandy clay soil. (C and D) Percentage contribution of path analysis coefficients to the correlation between σ_p and each C fraction. W, water content.

but the authors did not examine whether this correlation received contribution from water content or BD, which drive changes in soil compressibility (Schjønning & Lamandé, 2018). In examining soil compressibility parameters for a range of clay content in tropical soil as a function of organic carbon, BD, and water content, Reichert et al. (2018) found that increasing organic matter increases the soil compression index and reduces soil strength. However, the authors did not calculate the contribution of water content or BD to the correlation with organic carbon. Their results contrast with ours, in which an increase in organic matter correlated with soil compression index reduction, increasing compaction resistance. But our results corroborate those by Moraes et al. (2019), who observed gains in load-bearing capacity due to the strengthening of organic carbon bonds.

Precompression stress was the only indicator not affected by any organic carbon fraction. Imhoff et al. (2004) also found no influence of C on precompression stress, corroborating our findings. Reichert et al. (2018) and Toledo et al. (2021) reported a decreased precompression stress with soil organic carbon, whereas Moraes et al. (2019) suggested that the strengthening of C bonds was responsible for increases in precompression stress. Most of these results are unclear about the role of C on soil precompression stress—the direction of the correlation is ambiguous, as is the case for soil BD (positive) or water content (negative). Quantifying the effect of organic carbon on precompression stress is important because load-bearing capacity is extensively used as a measure for assessing the risk of compaction by pedo-transfer functions (Schjønning et al., 2022). Thus, knowing if soil C

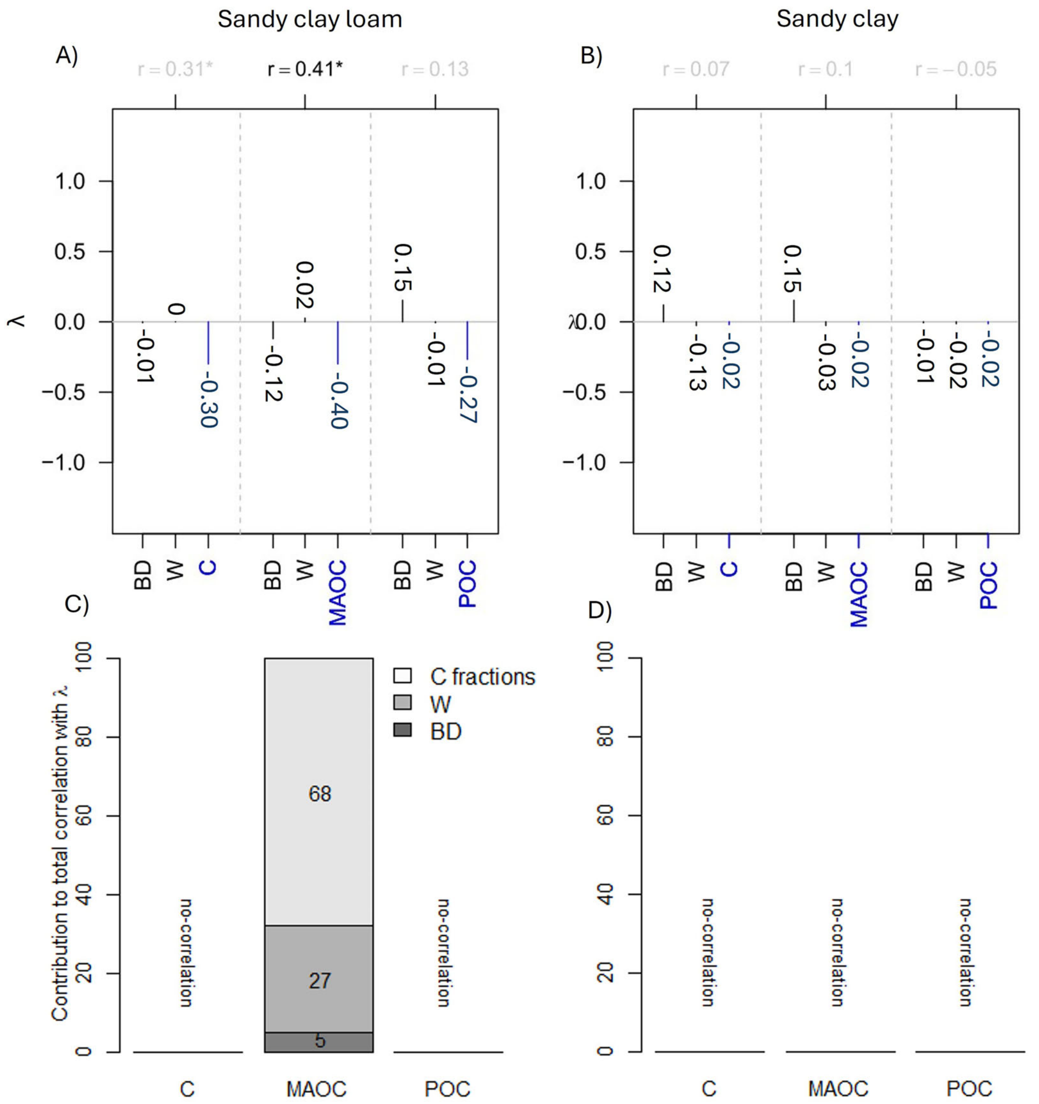

FIGURE 9 (A and B) Correlation (r) between the response variable λ (compression index) and total organic carbon and its fractions (organic carbon [C], mineral-associated organic carbon [MAOC], and particulate organic carbon [POC]). *$p < 0.05$. Vertical lines represent the estimates of path analysis coefficients. Blue lines indicate direct effects on λ. Black lines indicate indirect effects of soil bulk density (BD) and gravimetric water content (W) through each carbon fraction on the correlation for the sandy loam soil and sandy clay soil. (C and D) Percentage contribution of path analysis coefficients to the correlation between λ and each soil C fraction. W, water content.

should be considered when predicting precompression stress and what the real direction (negative or positive) of the effect is in predictive models is necessary. Our observations are limited to −100 hPa (despite a range of BD), and further studies should include lower matric potentials to compute possible interactions of organic matter with soil water content.

4.4 | Gains in SPR are related to increases in soil C

Increases in penetration resistance correlated with increases in soil C, with indirect effects of water content or BD. MAOC and POC increases lead to higher soil penetration resistance, corroborating Stock and Downes (2008). These authors observed that SPRincreased under matric potential below field capacity (i.e., dry range) by organic matter addition. They assumed that this strength gain derived from a cohesion gain induced by organic matter, agreeing with Horn (2004) and our results. Zhang and Hartge (1990) mixed organic matter with finer sand and observed no cohesion under saturated conditions with added organic matter, but organic matter enhanced the cohesion as soil dried. This indicates that SPR gain induced by organic matter could be more evident and detectable under unsaturated conditions or, more specifically, at water content below field capacity, in a mechanism induced by cohesion gain. Interestingly, however, this soil cohesion gain seems more prominent and significant in SPR or aggregate measurements than in soil compressibility indicators.

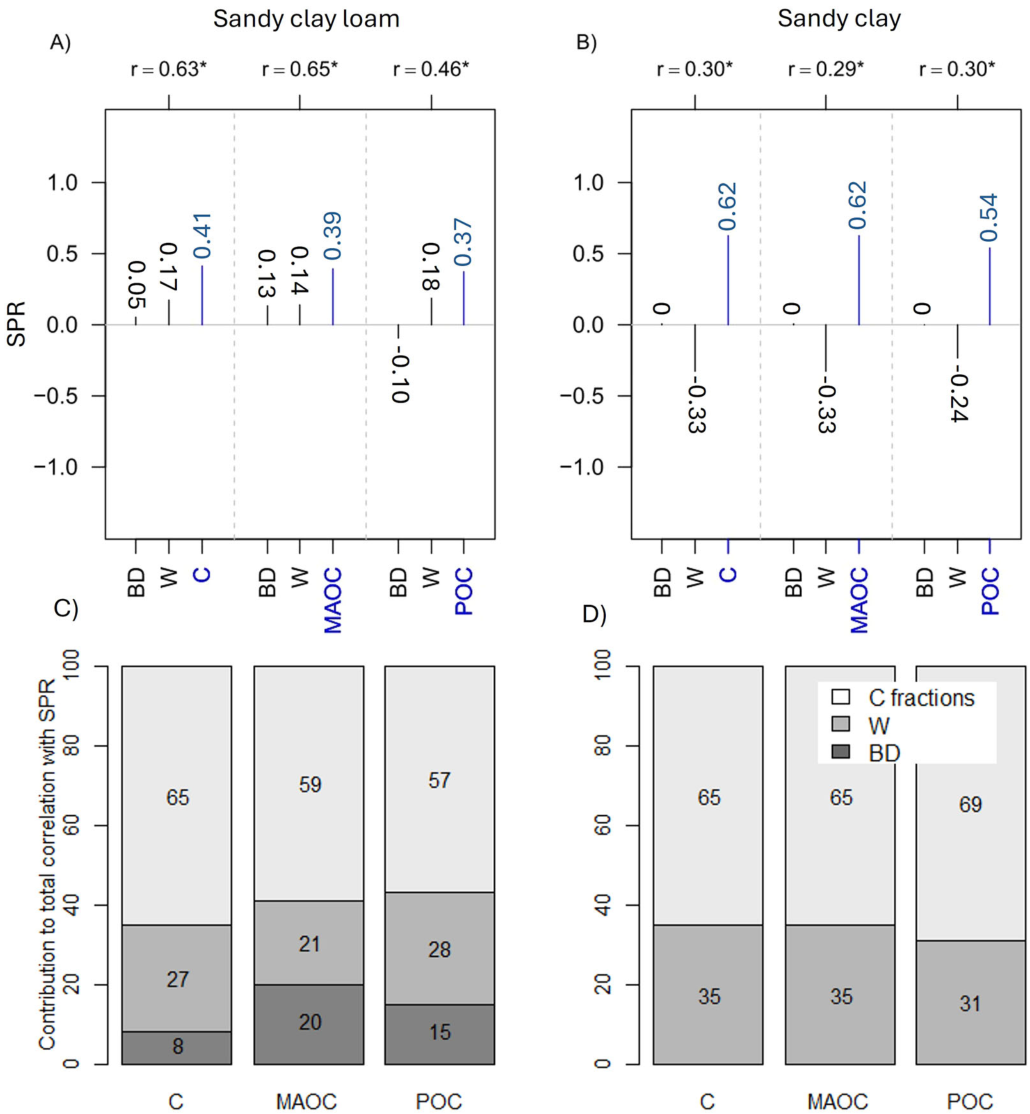

FIGURE 10 (A and B) Correlation (r) between the response variable SPR (soil penetration resistance) and total organic carbon and its fractions (organic carbon [C], mineral-associated organic carbon [MAOC], and particulate organic carbon [POC]). $*p < 0.05$. Vertical lines represent the estimates of path analysis coefficients. Blue lines indicate direct effects on SPR. Black lines indicate indirect effects of soil bulk density (BD) and gravimetric water content (W) through each carbon fraction on the correlation for the sandy loam soil and sandy clay soil. (C and D) Percentage contribution of path analysis coefficients to the correlation between SPR and each soil C fraction. W, water content.

According to Hadas and Lennard (1988), Mohr–Coulomb theory is used to determine the maximal shear stress or strength of porous materials like soils. It proposes an equation composed of frictional and cohesive forces, which Bengough (1992) uses to describe adhesion (instead of cohesive) forces involving penetrometers. Particle movement during cavity expansion by the penetrometer may also involve cohesive forces, which could be increased by increases in organic carbon (e.g., Stock & Downes, 2008; Zhang & Hartge, 1990). Over time, this increase in cohesion forces could be similar to the strengthening of carbon bonds reported by Moraes et al. (2017). Horn (2004) observed this phenomenon in conservation tillage fields by directly measuring cohesion (i.e., cohesion values). Logically, these same cohesive forces are present in the soils tested for aggregate and compressibility tests. For aggregates and penetration resistance tests, these cohesive forces induced by mineral-carbon bonds seem to be detectable by the induced failure process. Noting something similar was verified for compressibility, probably due to the nature of the compaction process, which is naturally related to void reduction.

4.5 | Overall observations on the role of soil C on mechanical strength gains

Our study hypothesized that C accumulation in soils without mechanical disturbance would induce mechanical strength gains, with a more pronounced role of mineral-associated organic matter. As isolating the role of carbon from water

TABLE 4 Qualitative description of the correlation between organic carbon fractions and soil strength indicators.

Soil	Carbon-induced effect	σ_t	σ_p	λ	SPR
Sandy clay loam	C				The higher the C, MAOC, or POC, the higher the soil penetration resistance. Effect 43%–33% mediated by water content and bulk density
	MAOC	The higher the MAOC, the higher the tensile strength. Effect 46% mediated by bulk density		The higher the MAOC, the lower the compression index. Effect 27% mediated by bulk density	
	POC				
Sandy clay	C MAOC POC	The higher the C, MAOC, or POC, the higher the tensile strength. Purely carbon-induced effect			The higher the C, MAOC, or POC, the higher the soil penetration resistance. Effect 35%–31% mediated by water content

Note: Green colors indicate correlation, whereas red colors indicate the absence of correlation.
Abbreviations: C, organic carbon; MAOC, mineral-associated soil organic carbon; POC, particulate soil organic carbon; SPR, soil penetration resistance; λ, soil compression index; σ_p, precompression stress; σ_t, tensile strength.

content or BD is difficult given its interaction with these factors in inducing strength, path analysis computed the impact of the partial correction attributed only to C and its fractions. Based on Moraes et al. (2017), our concern with the assumption that soil C could promote soil strength increase is the many existing indicators of soil strength (not just soil penetration resistance); thus measuring tensile strength, compressibility indicators and penetration resistance helps to verify whether this assumption is valid for other indicators. Our findings, summarized in Table 4, indicate that this theory is true, albeit limited. Given the clear scientific consensus that organic matter increases aggregate stability (Rabot et al., 2018), the question was whether this would extend to mechanical strength.

C plays an evident role in tensile strength gain considering soils with higher clay content, but this role is limited to mineral-associated organic matter in sandier soil. We also confirm the observations by Moraes et al. (2017), who noted a C-induced increase in soil penetrance resistance, which was measured for both soils studied. Interestingly, the fact that clay can naturally interact more strongly with organic matter to promote soil structure stabilization (or strength) (Wenzel et al., 2024) is more evident in measurements performed on aggregates (e.g., tensile strength).

5 | CONCLUSIONS

Soil organic C positively correlated with soil strength, indicating increased aggregate strength and soil penetration resistance. Organic C, in turn, had little influence on soil compressibility strength indicators. These findings indicate that the significant gains in aggregate soil stability and strength and penetration resistance induced by C are not completely transferred to soil compressibility measurements. Our results revealed that mineral-associated organic matter plays a positive role regarding soil strength gains in the coarse-textured soil, whereas all C fractions contribute to soil strength gains with increasing clay content. Soil C addition in the absence of soil mobilization may be beneficial for soil conservation given its influence on gains in aggregate stability and strength and on gains in SPR for root development. However, gains in compaction resistance should not be expected.

AUTHOR CONTRIBUTIONS

Renato P. de Lima: Conceptualization; data curation; formal analysis; methodology; software. **Cassio A. Tormena**: Conceptualization; investigation; methodology. **Rafael B. Menillo**: Data curation; formal analysis; methodology. **Newton La Scala Júnior**: Conceptualization; methodology. **Anderson R. da Silva**: Data curation; formal analysis. **Zigomar M. Souza**: Conceptualization; investigation; methodology. **Carlos E. P. Cerri**: Conceptualization; funding acquisition; investigation. **Maurício R. Cherubin**: Conceptualization; funding acquisition; investigation; methodology; project administration.

ACKNOWLEDGMENTS

Renato P. de Lima gratefully acknowledges the São Paulo Research Foundation (FAPESP, Grant No. 2020/15783-4) for providing a scholarship and the National Council for Scientific and Technological Development (CNPq, Grant No. 316751/2021-9 and 405784/2023-6) for financial support.

The Article Processing Charge for the publication of this research was funded by the Coordenação de Aperfeiçoamento de Pessoal de Nível Superior - Brasil (CAPES) (ROR identifier: 00x0ma614).

CONFLICT OF INTEREST STATEMENT

The authors declare no conflicts of interest.

ORCID

Renato P. de Lima https://orcid.org/0000-0003-0524-439X
Rafael B. Menillo https://orcid.org/0009-0001-0700-4499
Anderson R. da Silva https://orcid.org/0000-0003-2518-542X

REFERENCES

Akinwande, M. O., Dikko, H. G., & Samson, A. (2015). Variance inflation factor: As a condition for the inclusion of suppressor variable (s) in regression analysis. *Open Journal of Statistics*, *5*, 754. https://doi.org/10.4236/ojs.2015.57075

Bengough, A. G. (1992). Penetrometer resistance equation: Its derivation and the effect of soil adhesion. *Journal of Agricultural Engineering Research*, *53*, 163–168. https://doi.org/10.1016/0021-8634(92)80080-C

Bin, Z., & Xin-Hua, P. E. N. G. (2006). Organic matter enrichment and aggregate stabilization in a severely degraded ultisol after reforestation. *Pedosphere*, *16*, 699–706. https://doi.org/10.1016/S1002-0160(06)60105-7

Błażejczak, D., Horn, R., & Pytka, J. (1995). Soil tensile strength as affected by time, water content and bulk density. *International Agrophysics*, *9*(3), 179–188.

Blanco-Moure, N., Angurel, L. A., Moret-Fernández, D., & López, M. V. (2012). Tensile strength and organic carbon of soil aggregates under long-term no tillage in semiarid Aragon (NE Spain). *Geoderma*, *189*, 423–430. https://doi.org/10.1016/j.geoderma.2012.05.015

Cambardella, C. A., & Elliott, E. T. (1992). Particulate soil organic-matter changes across a grassland cultivation sequence. *Soil Science Society of America Journal*, *56*, 777–783. https://doi.org/10.2136/sssaj1992.03615995005600030017x

Cavalcanti, R. Q., Rolim, M. M., de Lima, R. P., Tavares, U. E., Pedrosa, E. M., & Cherubin, M. R. (2020). Soil physical changes induced by sugarcane cultivation in the Atlantic Forest biome, northeastern Brazil. *Geoderma*, *370*, 114353. https://doi.org/10.1016/j.geoderma.2020.114353

Cerri, C. E. P., Cerri, C. C., Maia, S. M. F., Cherubin, M. R., Feigl, B. J., & Lal, R. (2018). Reducing amazon deforestation through agricultural intensification in the Cerrado for advancing food security and mitigating climate change. *Sustainability*, *10*, 989. https://doi.org/10.3390/su10040989

Cotrufo, M. F., Haddix, M. L., Kroeger, M. E., & Stewart, C. E. (2022). The role of plant input physical-chemical properties, and microbial and soil chemical diversity on the formation of particulate and mineral-associated organic matter. *Soil Biology and Biochemistry*, *168*, Article 108648. https://doi.org/10.1016/j.soilbio.2022.108648

da Silva, A. R., Malafaia, G., & Menezes, I. P. P. (2017). Biotools: An R function to predict spatial gene diversity via an individual-based approach. *Genetics and Molecular Research*, *16*(2), 1–6. https://doi.org/10.4238/gmr16029655

da Silva, A. R., & de Lima, R. P. (2015). Soilphysics: an R package to determine soil preconsolidation pressure. *Computers & Geosciences*, *84*, 54–60.

da Silva, A. R., & de Lima, R. P. (2016). Comparison of methods for determining precompression stress based on computational simulation. *Revista Brasileira de Ciência do Solo*, *40*, e0150164.

da Silva, A. R., Nascimento, M., Cecon, P. R., Sapucay, M. J., do Rêgo, E. R., & Barbosa, L. A. (2013). Path analysis in multicollinearity for fruit traits of pepper. *IDESIA*, *31*(2), 55–60. https://doi.org/10.4067/S0718-34292013000200008

Dexter, A. R., Horn, R., & Kemper, W. D. (1988). Two mechanisms for age-hardening of soil. *Journal of Soil Science*, *39*, 163–175.

Dettmann, U., Kraft, N. N., Rech, R., Heidkamp, A., & Tiemeyer, B. (2021). Analysis of peat soil organic carbon, total nitrogen, soil water content and basal respiration: Is there a 'best'drying temperature?. *Geoderma*, *403*, 115231. https://doi.org/10.1016/j.geoderma.2021.115231

Dexter, A. R. (1988). Advances in characterization of soil structure. *Soil & Tillage Research*, *11*, 199–238. https://doi.org/10.1016/0167-1987(88)90002-5

Dexter, A. R. (1990). Changes in the matric potential of soil water with time after disturbance of soil by moulding. *Soil & Tillage Research*, *16(1-2)*, 35–50. https://doi.org/10.1016/0167-1987(90)90020-E

Dexter, A. R., & Kroesbergen, B. (1985). Methodology for determination of tensile strength of soil aggregates. *Journal of Agricultural Engineering Research*, *31*, 139–147. https://doi.org/10.1016/0021-8634(85)90066-6

Dexter, A. R., & Watts, C. W. (2000). Tensile strength and friability. In *Soil and environmental analysis* (pp. 417–446). CRC Press.

Figueiredo, G. C., Silva, A. P., Tormena, C. A., Giarola, N. F. B., Moraes, S. O., & Almeida, B. G. (2011). Desenvolvimento de um consolidômetro pneumático: Modelagem da compactação, penetrometria e resistência tênsil de agregados de solo. *Revista Brasileira de Ciência do Solo*, *35*, 389–402. https://doi.org/10.1590/S0100-06832011000200009

Hadas, A., & Lennard, G. (1988). Dependence of tensile strength of soil aggregates on soil constituents, density and load history. *Journal of Soil Scssience*, *39*, 577–586. https://doi.org/10.1111/j.1365-2389.1988.tb01241.x

Hillel, D. (2003). *Introduction to environmental soil physics*. Elsevier.

Horn, R. (2004). Time dependence of soil mechanical properties and pore functions for arable soils. *Soil Science Society of America Journal*, *68*(4), 1131–1137. https://doi.org/10.2136/sssaj2004.1131

Horn, R., & Fleige, H. (2011). Soil structure and mechanical strength. In J. Gliński, J. Horabik, & J. Lipiec (Eds.), *Encyclopedia of agrophysics. Encyclopedia of earth sciences series* (pp. 777–780). Springer.

Imhoff, S., Da Silva, A. P., & Dexter, A. (2002). Factors contributing to the tensile strength and friability of Oxisols. *Soil Science Society of America Journal*, *66*, 1656–1661. https://doi.org/10.2136/sssaj2002.1656

Imhoff, S., Da Silva, A. P., & Fallow, D. (2004). Susceptibility to compaction, load support capacity, and soil compressibility of Hapludox. *Soil Science Society of America Journal*, *68*, 17–24. https://doi.org/10.2136/sssaj2004.1700

Islam, M. R., Singh, B., & Dijkstra, F. A. (2022). Stabilisation of soil organic matter: Interactions between clay and microbes. *Biogeochemistry*, *160*, 145–158. https://doi.org/10.1007/s10533-022-00956-2

Keller, T., Lamandé, M., Schjønning, P., & Dexter, A. R. (2011). Analysis of soil compression curves from uniaxial confined compression tests. *Geoderma*, *163*, 13–23. https://doi.org/10.1016/j.geoderma.2011.02.006

Kunde, R. J., Lima, C. L. R. D., Silva, S. D. D. A., & Pillon, C. N. (2018). Tensile strength, friability, aggregation, and soil organic matter physical fractions of an Oxisol cultivated with sugarcane. *Pesquisa Agropecuária Brasileira*, *53*, 487–494. https://doi.org/10.1590/s0100-204x2018000400010

Lavallee, J. M., Soong, J. L., & Cotrufo, M. F. (2020). Conceptualizing soil organic matter into particulate and mineral-associated forms to address global change in the 21st century. *Global Change Biology*, *26*, 261–273.

Moraes, M. T., da Luz, F. B., Debiasi, H., Franchini, J. C., & da Silva, V. R. (2019). Soil load support capacity increases with time without soil mobilization as a result of age-hardening phenomenon. *Soil & Tillage Research*, *186*, 128–134. https://doi.org/10.1016/j.still.2018.09.009

Moraes, M. T., Debiasi, H., Carlesso, R., Franchini, J. C., da Silva, V. R., & da Luz, F. B. (2017). Age-hardening phenomena in an Oxisol from the subtropical region of Brazil. *Soil & Tillage Research*, *170*, 27–37. https://doi.org/10.1016/j.still.2017.03.002

Or, D., & Ghezzehei, T. A. (2002). Modeling post-tillage soil structural dynamics: A review. *Soil & Tillage Research*, *64*(1–2), 41–59. https://doi.org/10.1016/S0167-1987(01)00256-2

Pereira, J. O., Défossez, P., & Richard, G. (2007). Soil susceptibility to compaction by wheeling as a function of some properties of a silty soil as affected by the tillage system. *European Journal of Soil Science*, *58*, 34–44. https://doi.org/10.1111/j.1365-2389.2006.00798.x

Pesch, C., Lamandé, M., de Jonge, L. W., Norgaard, T., Greve, M. H., & Moldrup, P. (2020). Compression and rebound characteristics of agricultural sandy pasture soils from South Greenland. *Geoderma*, *380*, 114608. https://doi.org/10.1016/j.geoderma.2020.114608

Prairie, A. M., King, A. E., & Cotrufo, M. F. (2023). Restoring particulate and mineral-associated organic carbon through regenerative agriculture. *Proceedings of the National Academy of Sciences*, *120*(21), e2217481120. https://doi.org/10.1073/pnas.2217481120

Rabot, E., Wiesmeier, M., Schlüter, S., & Vogel, H. J. (2018). Soil structure as an indicator of soil functions: A review. *Geoderma*, *314*, 122–137.

R Core Team. (2022). *R: A language and environment for statistical computing*. R Foundation for Statistical Computing. http://www.Rproject.org

Reichert, J. M., Mentges, M. I., Rodrigues, M. F., Cavalli, J. P., Awe, G. O., & Mentges, L. R. (2018). Compressibility and elasticity of subtropical no-till soils varying in granulometry organic matter, bulk density and moisture. *Catena*, *165*, 345–357. https://doi.org/10.1016/j.catena.2018.02.014

Saffih-Hdadi, K., Défossez, P., Richard, G., Cui, Y. J., Tang, A. M., & Chaplain, V. (2009). A method for predicting soil susceptibility to the compaction of surface layers as a function of water content and bulk density. *Soil & Tillage Research*, *105*, 96–103. https://doi.org/10.1016/j.still.2009.05.012

Salire, E. V., Hammel, J. E., & Hardcastle, J. H. (1994). Compression of intact subsoils under short-duration loading. *Soil & Tillage Research*, *31*(2–3), 235–248. https://doi.org/10.1016/0167-1987(94)90083-3

Schjønning, P., & Lamandé, M. (2018). Models for prediction of soil precompression stress from readily available soil properties. *Geoderma*, *320*, 115–125. https://doi.org/10.1016/j.geoderma.2018.01.028

Schjønning, P., Lamandé, M., De Pue, J., Cornelis, W. M., Labouriau, R., & Keller, T. (2022). The challenge in estimating soil compressive strength for use in risk assessment of soil compaction in field traffic. Advances in agronomy. *Advances in Agronomy*, *178*, 61–105.

Schjønning, P., van den Akker, J. J., Keller, T., Greve, M. H., Lamandé, M., Simojoki, A., Stettler, M., Arvidsson, J., & Breuning-Madsen, H. (2015). Driver-pressure-state-impact-response (DPSIR) analysis and risk assessment for soil compaction—A European perspective. *Advances in Agronomy*, *133*, 183–237.

Singh, M., Sarkar, B., Biswas, B., Bolan, N. S., & Churchman, G. J. (2017). Relationship between soil clay mineralogy and carbon protection capacity as influenced by temperature and moisture. *Soil Biology and Biochemistry*, *109*, 95–106. https://doi.org/10.1016/j.soilbio.2017.02.003

Six, J., Bossuyt, H., Degryze, S., & Denef, K. (2004). A history of research on the link between (micro) aggregates, soil biota, and soil organic matter dynamics. *Soil & Tillage Research*, *79*, 7–31. https://doi.org/10.1016/j.still.2004.03.008

Soil Survey Staff. (2014). *Keys to soil taxonomy* (12th ed.). NRCS.

Startsev, V. V., Khaydapova, D. D., Degteva, S. V., & Dymov, A. A. (2020). Soils on the southern border of the cryolithozone of European part of Russia (the Subpolar Urals) and their soil organic matter fractions and rheological behavior. *Geoderma*, *361*, Article 114006. https://doi.org/10.1016/j.geoderma.2019.114006

Stock, O., & Downes, N. K. (2008). Effects of additions of organic matter on the penetration resistance of glacial till for the entire water tension range. *Soil & Tillage Research*, *99*, 191–201. https://doi.org/10.1016/j.still.2008.02.002

Stumpf, L., dos Anjos Leal, O., Pauletto, E. A., Pinto, L. F. S., Reis, D. A., Pinto, M. A. B., & Tuchtenhagen, I. K. (2018). Tensile strength and organic matter fractions in aggregates of a grass-covered mined soil under early stage recovery. *Soil & Tillage Research*, *176*, 69–76. https://doi.org/10.1016/j.still.2017.11.006

Toledo, M. P., Rolim, M. M., de Lima, R. P., Cavalcanti, R. Q., Ortiz, P. F., & Cherubin, M. R. (2021). Strength, swelling and compressibility of unsaturated sugarcane soils. *Soil & Tillage Research*, *212*, Article 105072. https://doi.org/10.1016/j.still.2021.105072

Trumbore, S. E., Davidson, E. A., Barbosa de Camargo, P., Nepstad, D. C., & Martinelli, L. A. (1995). Belowground cycling of carbon in forests and pastures of Eastern Amazonia. *Global Biogeochemical Cycles*, *9*, 515–528.

van Lier, Q. D. J. (2017). Field capacity, a valid upper limit of crop available water? *Agricultural Water Management*, *193*, 214–220. https://doi.org/10.1016/j.agwat.2017.08.017

Wenzel, W. W., Golestanifard, A., & Duboc, O. (2024). SOC: Clay ratio: A mechanistically-sound, universal soil health indicator across ecological zones and land use categories? *Geoderma*, *452*, 117080. https://doi.org/10.1016/j.geoderma.2024.117080

Zhang, H. Q., & Hartge, K. H. (1990). Cohesion in unsaturated sandy soils and the influence of organic matter. *Soil Technology*, *3*, 31–326. https://doi.org/10.1016/0933-3630(90)90013-S

How to cite this article: de Lima, R. P., Tormena, C. A., Menillo, R. B., La Scala Júnior, N., da Silva, A. R., Souza, Z. M., Cerri, C. E. P., & Cherubin, M. R. (2025). Correlation of total organic C, particulate and mineral-associated C fractions with strength indicators in Oxisols. *Soil Science Society of America Journal*, *89*, e70141. https://doi.org/10.1002/saj2.70141